NUCLEAR SCIENCE AND ENGINEERING: **127**, 230–237 (1997)

Technical Note

Neutron Skyshine Calculations with the Integral Line-Beam Method

Ah Auu Gui, J. Kenneth Shultis,* and Richard E. Faw

Kansas State University, Department of Nuclear Engineering, Manhattan, Kansas 66506-2503

Received September 16, 1996
Accepted March 4, 1997

Abstract—*Recently developed line- and conical-beam response functions are used to calculate neutron skyshine doses for four idealized source geometries. These calculations, which can serve as benchmarks, are compared with MCNP calculations, and the excellent agreement indicates that the integral conical- and line-beam method is an effective alternative to more computationally expensive transport calculations.*

I. INTRODUCTION

Accurate calculation of the neutron and secondary-photon skyshine doses is a difficult computational challenge, especially at large distances from the neutron source. To reduce the computational effort, several simplified methods have been developed. One of these methods, the integral line-beam method, has been applied to both gamma-photon and neutron skyshine problems. The efficacy of this method has been well established for the gamma-photon skyshine problem.[1–7]

Although the integral line-beam method can also be applied to the neutron skyshine problem,[1,2] comparisons of results with other benchmark calculations are few, and they are complicated by the variety of different dosimetric units used in past neutron skyshine calculations. Conversion between two neutron dosimetric units generally requires knowledge of the neutron energy spectrum, information which generally is unreported. In this paper we use recently developed response functions for both the neutron and secondary-photon skyshine doses in the integral line-beam method and compare the results (expressed in modern dosimetric units) with results obtained with the MCNP code.

II. THE INTEGRAL LINE-BEAM METHOD

The integral line-beam method is based on two key approximations. The first is that the neutron source can be treated as a point source and that the source containment structure causes a negligible perturbation on the skyshine radiation field. Once source radiation enters the atmosphere, it does not interact again with the source structure, and, consequently, the energy and angular distribution of source radiation penetrating any overhead source shield or escaping from the containment structure is independent of the subsequent transport of the radiation through the air to the detector. In most skyshine calculations at distances far from the source, the source and its containment have a negligible effect on the transport of the radiation through the air once the radiation has left the source structure.[5]

The second key approximation is that the effect of the air-ground interface is negligible and that the ground can be replaced by a continuation of the infinite-air medium. Neglect of the air-ground interface introduces little error for gamma-ray skyshine,[8] and for neutron skyshine problems it is usually conservative[9,10] except at very small source-to-detector distances, when the presence of the ground acts as a reflector to the skyshine and increases the radiation dose.

The integral line-beam method is based on the availability of a line-beam response function (LBRF). The LBRF $\Re_i(E, x, \phi)$ is the expected neutron skyshine dose at a point isotropic detector in an infinite homogeneous air medium a distance x from a point source that emits a neutron with energy E at an angle ϕ with respect to the source-detector axis. The subscript i refers to the dose from neutrons ($i = n$) or from secondary photons ($i = p$). The skyshine dose rate $R_i(x)$ at a detector a distance x from a collimated point source that emits $S(E, \mathbf{\Omega})\, dE\, d\Omega$ neutrons per unit time with energies in dE

*E-mail: jks@ksu.edu.

about E into directions $d\Omega$ about $\mathbf{\Omega}$ is found by integrating the LBRF over all source energies and over all radiation emission directions allowed by any source collimation, namely,

$$R_i(x) = \int_0^\infty dE \int_0^{2\pi} d\psi \int_0^{\theta_{max}(\psi)} d\theta \sin\theta S[E,\mathbf{\Omega}(\theta,\psi)] \times \Re_i[x,E,\phi(\theta,\psi)] \ . \quad (1)$$

Here θ and ψ are the polar and azimuthal angles of $\mathbf{\Omega}$ in a spherical coordinate system centered at the source and with the upward vertical as the polar axis. The emission angle ϕ is related to θ and ψ by[4,6]

$$\cos\phi = \mathbf{\Omega}\cdot\boldsymbol{u} = \sin\theta\cos\psi\cos\zeta + \cos\theta\sin\zeta \ , \quad (2)$$

where $\mathbf{\Omega}$ is a unit vector in the neutron emission direction, $\boldsymbol{u}$ is a unit vector from the source toward the detector, and $\zeta = \tan^{-1}(h/x)$, in which h is the detector height less the source height. For a shielded source, $S(E,\mathbf{\Omega})$ in Eq. (1) describes the neutrons penetrating the shield into the atmosphere.

For the special case where the source is symmetric about the azimuth, i.e., $S(E,\mathbf{\Omega}) \rightarrow S(E,\theta)$, and the source and detector are at the same elevation, the skyshine dose of Eq. (1) for an infinite-air medium reduces to

$$R_i(x) = 2\pi \int_0^\infty dE \int_0^{\theta_{max}} d\theta \sin\theta \, S(E,\theta)\Re_{ci}(x,E,\theta) \ , \quad (3)$$

in which the conical-beam response function (CBRF) $R_{ci}(x,E,\theta)$ is related to the LBRF by

$$\Re_{ci}(x,E,\theta) = \frac{1}{2\pi}\int_0^{2\pi} d\psi \, \Re_i(x,E,\phi) \ , \quad (4)$$

where $\phi = \cos^{-1}(\sin\theta\cos\psi)$.

The angular integrals in Eqs. (1) and (3) are readily evaluated numerically by using Monte Carlo methods[1,2] or by using standard numerical quadrature.[3–7] The integration over the source energy is usually treated by a discretization approximation wherein source neutrons are assigned to energy bins, each of which is treated separately as a monoenergetic source. The results for each bin are then summed to give the total skyshine dose.

II.A. Approximation of the Response Functions

Critical to the integral line-beam method is a simple approximation of the LBRF and the CBRF. It has been found that the neutron and secondary-photon LBRFs can be approximated well for neutron source energies from 0.01 to 14 MeV in air of density ρ by[1,10]

$$\Re_i(x,E,\phi) = E(\rho/\rho_o)^2(\rho x/\rho_o)^c \times \exp(a + b\rho x/\rho_o) \ , \quad i = n,p \ . \quad (5)$$

Here the reference density $\rho_o = 1.20$ g/ℓ.

Although the CBRF may be calculated numerically from Eq. (4) using the approximate LBRF of Eq. (5) and numerical integration, it is more efficient in integral line-beam calculations to use directly an approximation of the neutron and secondary-photon CBRFs. For source neutrons with energies between 0.01 and 14 MeV, the secondary-photon CBRF $\Re_{cp}(x,E,\theta)$ can be approximated by the empirical function of Eq. (5). The neutron CBRF can be approximated by[10]

$$\Re_c(x,E,\theta) = E(\rho/\rho_o)^2 e^a (\rho x/\rho_o)^{b(\rho x/\rho_o)+c} \ . \quad (6)$$

Compilations of the parameters a, b, and c in these approximations for 14 discrete energies between 0.01 and 14 MeV and for multiple emission angles are available.[11,12] The compilations give the skyshine dose in three modern dosimetric units, namely, the effective dose equivalent for an anthropomorphic phantom (AP iradiation geometry) and the dose equivalents on the principal axis at a depth of 10 mm for radiation incident in plane parallel beam (PAR) and isotropic (ISO) irradiation geometries on the ICRU sphere. The fluence-to-dose conversion factors were taken from Ref. 13. A double interpolation scheme can be used to make these approximations continuous in all three independent variables.[10]

III. APPLICATION TO THREE SIMPLE SKYSHINE PROBLEMS

In this section, the use of recently developed approximate response functions[11,12] for the neutron skyshine problem is demonstrated and results are compared with MCNP calculations for a point isotropic monoenergetic neutron source in four idealized skyshine geometries. For such a source, $S(E',\mathbf{\Omega}) = S_n\delta(E' - E)/4\pi$, where E is the energy of source neutrons and S_n is the source strength. The energy integrals in Eqs. (1) and (3) are thus avoided. The four geometries considered in this technical note are (a) a source on the axis of a roofless cylindrical shield (open silo), (b) a source behind an infinite-wall shield, (c) a source inside a roofless rectangular shield, and (d) a point isotropic source in an infinite-air medium. All of the shields collimating the sources are assumed to be black; that is, all neutrons or photons reaching the shields are completely absorbed.

The MCNP (Ref. 14) calculations were performed using version 4A and the ENDF/B-V cross sections distributed with the code. The integral line-beam calculations were performed with the SKYNEUT code,[15] which uses the response functions recently developed by Shultis and Faw[11] and Gui, Shultis, and Faw.[10] For all calculations, dry air of mass density 1.20 g/ℓ at 20°C and 1 atm was specified with the ANSI-6.4.3 (Ref. 16) composition, which is, by mass fraction, nitrogen 0.75519, oxygen 0.23179, carbon 0.00014, and argon 0.01288. The effect of the air-ground interface was neglected, with all

calculations being based on an infinite-air medium. Perturbations caused by the air-ground interface and air humidity are discussed elsewhere.[9,10]

The dose unit employed in all the following examples is the effective dose equivalent for an anthropomorphic phantom (AP irradiation geometry) with the fluence-to-dose conversion factors taken from Ref. 13. However, it should be noted that the neutron (but not the secondary-photon) dose is also multiplied by a factor of 2 as recommended in Ref. 17. This doubling of the ICRP-51 neutron dose is in conflict with current U.S. regulatory practice, which rejects the ICRP-45 recommendation and uses unmodified NCRP-38 conversion factors.[18]

III.A. Open-Silo Geometry

In this problem, a point isotropic monoenergetic neutron source is shielded by a roofless cylindrical black wall (silo) of inner radius r, as shown in Fig. 1. The source, which emits monoenergetic neutrons of energy E, is located on the axis of the silo at a vertical distance h_s below the silo top. A detector is located at a vertical distance h_d below the silo top and at a radial distance x from the silo axis. For this problem, a positive h_s (or h_d) denotes the source (or detector) is below the silo top, while a negative h_s (or h_d) denotes the source (or detector) is above the silo top. For this geometry with azimuthal symmetry, Eq. (1) simplifies to give the skyshine dose at a distance d from the source as

$$R_i(d) = \frac{S_n}{2\pi} \int_0^{\pi} d\psi \int_{\omega_o}^{1} d\omega \, \Re_i(d, E, \phi) \ , \qquad (7)$$

where $\omega \equiv \cos\theta$, $\omega_o = \cos\theta_{max}$, and θ_{max} is the maximum polar angle at which neutrons can escape the silo.

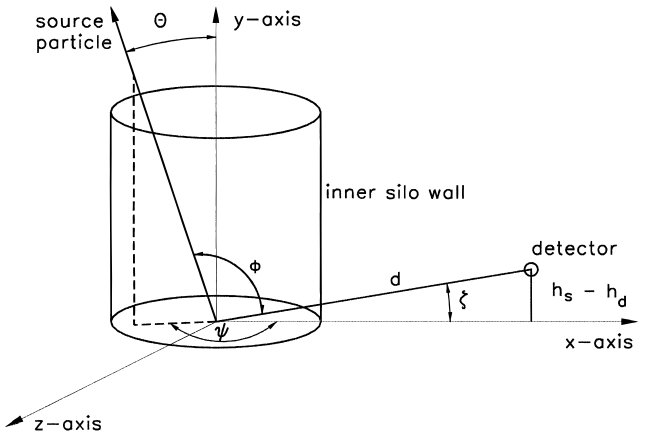

Fig. 1. Geometry for the open-silo skyshine problem. The point source is on the silo axis at the origin of the spherical coordinate system and at a vertical distance h_s below the silo top. A detector is located at $(x, h_s - h_d, 0)$. The silo wall is assumed to be black.

The subscript i denotes the skyshine dose attributed to the radiation of type i ($i = n$ for neutrons, and $i = p$ for secondary photons). For this geometry, $\cos\phi$ is given by Eq. (2), and

$$d = [x^2 + (h_s - h_d)^2]^{1/2} \ , \qquad (8)$$

$$\zeta = \tan^{-1}[(h_s - h_d)/x] \ , \qquad (9)$$

and

$$\omega_o \equiv \cos\theta_{max} = h_s/(r^2 + h_s^2)^{1/2} \ . \qquad (10)$$

Figures 2 and 3 compare the skyshine dose calculated by the MCNP code with that determined using the integral line-beam method. The results shown are for an open silo of 2-m inner radius, with the source and the detector at the same elevation ($h_s = h_d = 1$ m). The excellent agreement between the two sets of results shows that the integral line-beam method could be used to estimate the skyshine dose economically with acceptable accuracy.

It can be seen from Fig. 2 that the line-beam method results agreed very well with the MCNP results for neutrons with energy ≥3.25 MeV. For the 3.25-MeV neutrons, the MCNP results for the secondary photons at $x \leq 300$ m are not shown because their relative errors exceed 20%, higher than the maximum recommended value of 10% (Ref. 14). Figure 3 illustrates the effect of changing the source elevation. As expected, the skyshine dose decreases as the source is lowered into the silo. For

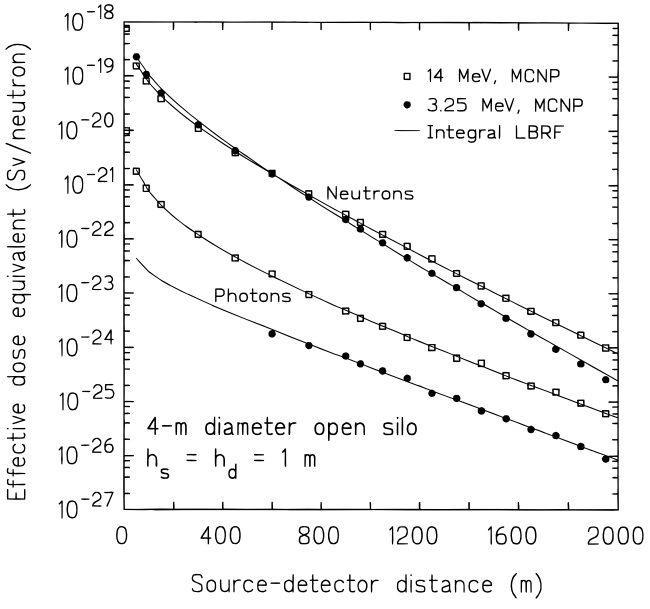

Fig. 2. Comparison of the MCNP and integral line-beam method results for an open silo of 2-m inner radius. Results shown are for point isotropic monoenergetic neutron sources on the silo axis and 1 m below the silo top. The point isotropic detector is also 1 m below the silo top.

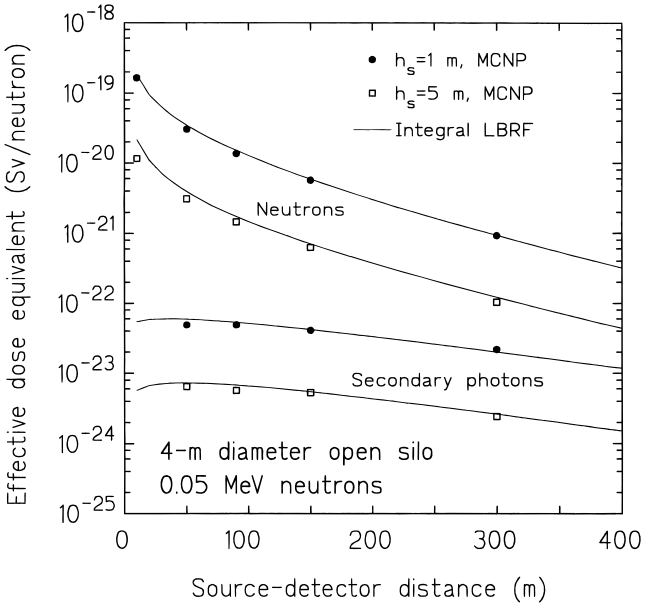

Fig. 3. Comparison of the MCNP and integral line-beam results for an open silo of 2-m inner radius. Results shown are for 0.05-MeV point isotropic neutron sources at 1 and 5 m below the silo top and on the silo axis. For both cases, $h_d = h_s$.

0.05-MeV neutrons, the integral line-beam method results based on the approximate LBRFs are slightly higher than the MCNP results at $x \leq 300$ m. The secondary-photon dose decreases as x decreases at $x \leq 150$ m. This is because the neutron energy is below the inelastic scattering thresholds for oxygen and nitrogen. In addition, at this distance, only a small fraction of the source neutrons are thermalized and are thus available for the production of capture gamma radiations.

The calculated skyshine dose using the integral line-beam method only accounts for the skyshine dose due to neutrons emitted from the source with a polar angle $\theta \leq \theta_{max}$ (i.e., $\omega \geq \cos\theta_{max}$), which is determined by the silo wall. Contributions from neutrons emitted with a polar angle $\geq \theta_{max}$ that first scatter from the silo wall and then reach the detector are neglected. However, this underestimation is compensated somewhat by neglecting the shielding of neutrons emitted with a polar angle $\theta \leq \theta_{max}$ and that are scattered by air inside the silo before traveling skyward. These simplifications, however, do not cause serious error in the far-field skyshine dose.[6]

Because the silo problem has azimuthal symmetry, the skyshine dose can be evaluated from Eq. (3) using the CBRF. For this monoenergetic silo problem, Eq. (3) reduces to

$$R_i(d) = \frac{S_n}{2} \int_{\omega_o}^{1} d\omega \, \Re_{ci}(d, E, \theta) \ . \qquad (11)$$

This equation is readily evaluated numerically using Gaussian quadrature. Figure 4 presents the results evaluated for neutron sources (14- and 3.25-MeV) on the vertical axis of a silo (2-m inner radius) and located 1 m below the silo top. Also shown are the previous results obtained from MCNP and integral line-beam method calculations. As expected, excellent agreement among the three sets of results is obtained. However, the integral conical-beam method results are closer to the MCNP results than those obtained using the integral line-beam method. For the 3.25-MeV neutrons, the LBRF overestimates the secondary-photon dose at source-detector distance $x \leq 500$ m. Actually, both the LBRF and the CBRF for the secondary photons produced by the 3.25-MeV source neutrons are not very accurate for $x \leq 300$ m, and their use at these distances should be undertaken with caution. Fortunately, because the secondary-photon doses at these distances are normally $<1\%$ of the total dose, their use will not result in serious error in the total skyshine dose.

III.B. Infinite-Wall Geometry

Figure 5 depicts the geometry of the skyshine problem for a point isotropic monoenergetic neutron source located at a perpendicular distance r behind an infinite black wall and at a vertical distance h_s measured from the horizontal plane touching the top of the wall. A detector, located on the opposite side of the wall, is at a horizontal distance z_d measured normally from the x axis and at a vertical distance h_d beneath the same horizontal plane through the top of the wall. For this geometry, Eq. (1) reduces to

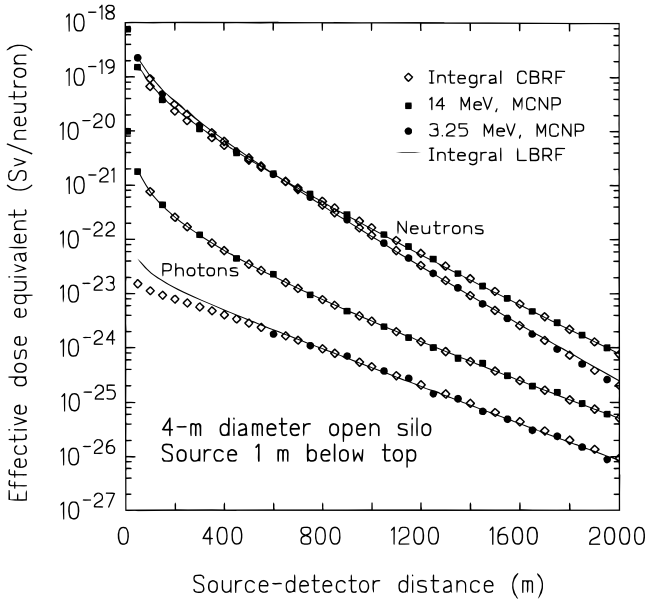

Fig. 4. Integral conical-beam method results for the open-silo skyshine problem. Also shown are results of Fig. 2 obtained using the integral line-beam method and results calculated directly using the MCNP code.

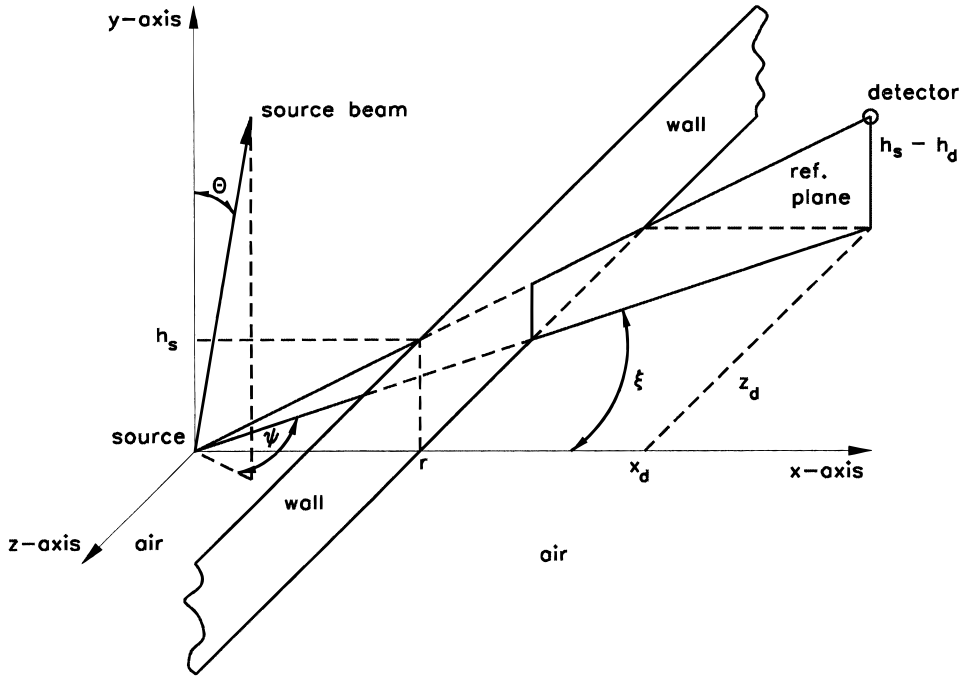

Fig. 5. Geometry for the infinite black wall problem. A point isotropic neutron source is located at a distance r behind the wall and a vertical distance h_s below the top of the wall. A detector is located at $(x_d, h_s - h_d, z_d)$, while the source is located at the origin of the coordinate system.

$$R_i(d) = \frac{S_n}{4\pi} \int_0^{2\pi} d\psi \int_{\omega_{min}}^{1} d\omega \, \Re_i(d, E, \phi) \ , \qquad (12)$$

where E is the energy of the neutrons emitted by the monoenergetic source. As before, the subscript i is used to denote the radiation type. This geometry has been analyzed by Shultis, Faw, and Deng[6] for the gamma-ray skyshine problem, and they have shown that

$$d = [x_d^2 + (h_s - h_d)^2 + z_d^2]^{1/2} \qquad (13)$$

and

$$\zeta = \tan^{-1}\left[\frac{h_s - h_d}{(x_d^2 + z_d^2)^{1/2}} \right] . \qquad (14)$$

Because the minimum value of θ is 0 deg, the upper limit of ω, $\omega_{max} = \cos\theta_{min}$, is equal to 1. The determination of $\omega_{min} = \cos\theta_{max}$ is slightly more involved. When the radiations are emitted in the direction toward the detector, that is, for the intervals $(0 \le \psi \le \pi/2 + \xi)$ and $(3\pi/2 + \xi \le \psi \le 2\pi)$ where $\xi = \tan^{-1}(z_d/x_d)$, θ_{max} occurs when the beam just grazes the top of the wall. For these ranges, $\theta_{max} = \tan^{-1}\{r/[h_s \cos(\psi - \xi)]\}$. When the radiations are emitted away from the detector, that is, for the range $(\pi/2 + \xi \le \psi \le 3\pi/2 + \xi)$, it is assumed that all radiations emitted contribute to the skyshine dose and θ_{max} becomes $\pi/2$ (or $\omega_{min} = 0$). Thus, the θ_{max} for the infinite-wall geometry is given by

$$\theta_{max} = \begin{cases} \tan^{-1}\left[\dfrac{r}{h_s \cos(\psi - \xi)} \right] , \\ \qquad 0 \le \psi \le \pi/2 + \xi, \\ \qquad 3\pi/2 + \xi \le \psi \le 2\pi \ , \\ \pi/2 \ , \quad \pi/2 + \xi \le \psi \le 3\pi/2 + \xi \ . \end{cases} \qquad (15)$$

The assumption that all of the radiations emitted in the direction away from the wall contribute to the skyshine dose tends to overestimate the actual skyshine dose because the initial portion of these backward beams is shielded by the infinite wall. However, because the contribution of the shielded portion of the backward beams is much smaller than the contribution from beams that are emitted toward the detector, the error due to the above assumption is usually small.[6]

Figure 6 presents the skyshine dose evaluated using the integral line-beam method together with the results calculated using the MCNP code. The results shown are for a 14-MeV point isotropic neutron source located at 1 m behind the infinite black wall and with a horizontal offset z_d of 0 m for three values of h_s ($h_s = h_d$): 0, 0.5, and 1 m. Again the agreement is remarkably good.

III.C. Open-Roof Rectangular Building Geometry

Most radiation facilities are normally well shielded on the sides, while much less shielding is provided by

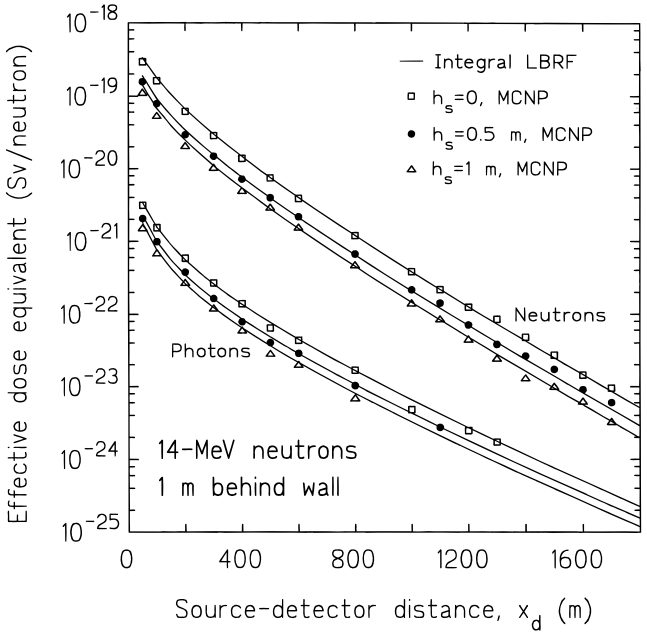

Fig. 6. Comparison of the MCNP (symbols) and the integral line-beam method results (lines) for the infinite-wall skyshine problem. The results are for a 14-MeV point isotropic neutron source located 1 m behind an infinite black wall and at a horizontal offset z_d of 0 m for three vertical distances below the top of the wall: h_s = 0, 0.5, and 1 m. In each case, the detector is at the source elevation.

the roof. Hence, the geometry analyzed here is of practical significance. The geometry of the problem is depicted in Fig. 7. A point isotropic monoenergetic neutron source is located on the z axis at a vertical distance h_s below the horizontal plane through the top of the roof. The front and rear walls are located at distances x_2 and x_1, respectively, from the source. The right wall of the building is located at a distance y_1 from the source along the y axis, while the left wall is located at a distance y_2 from the source. A detector is placed at the coordinate $(x_d, y_d, h_s - h_d)$. For this geometry, the skyshine dose for radiation of type i at the detector is given by

$$R_i(d) = \frac{S_n}{4\pi} \int_0^{2\pi} d\psi \int_{\omega_{min}(\psi)}^{1} d\omega \, \Re_i(d, E, \phi) \ . \quad (16)$$

In Eq. (16), ω_{min} is a function of the azimuthal angle ψ. It can be shown that the following relations hold:

$$d = [(x_2 + x_d)^2 + (h_s - h_d)^2 + y_d^2]^{1/2} \quad (17)$$

and

$$\zeta = \tan^{-1}\left\{ \frac{h_s - h_d}{[(x_2 + x_d)^2 + y_d^2]^{1/2}} \right\} \ . \quad (18)$$

The angle between the emission direction and the source-detector axis, ϕ, is still given by Eq. (2).

As for the infinite-wall case, it is obvious that the minimum value of the polar angle θ is 0 deg; thus $\omega_{max} = 1$. There are four possible values for θ_{max}, which occur when the source beam just clears the top corners of the rectangular room. With $\xi = \tan^{-1}[y_d/(x_2 + x_d)]$, the azimuthal angles corresponding to these four values are denoted by ψ_1, ψ_2, ψ_3, and ψ_4, which can be shown to be[6]

$$\psi_1 = \tan^{-1}(y_1/x_2) - \xi \ , \quad (19)$$

$$\psi_2 = \tan^{-1}(x_1/y_1) + \pi/2 - \xi \ , \quad (20)$$

$$\psi_3 = \tan^{-1}(y_2/x_1) + \pi - \xi \ , \quad (21)$$

and

$$\psi_4 = \tan^{-1}(x_2/y_2) + 3\pi/2 - \xi \ , \quad (22)$$

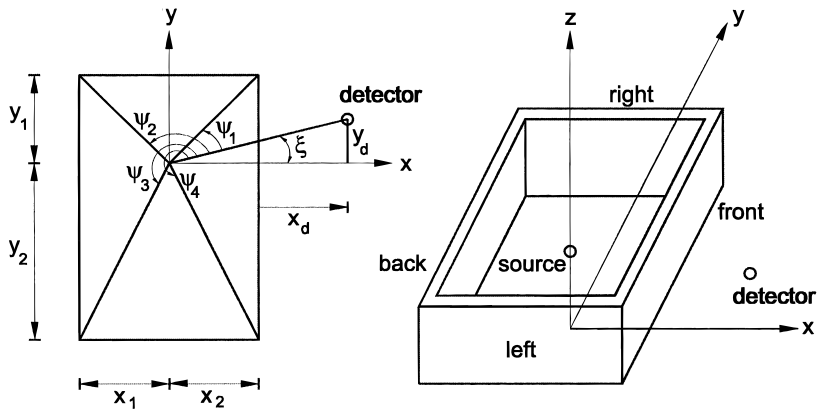

Fig. 7. Geometry for roofless rectangular building. The source is on the z axis at a vertical distance h_s below the horizontal plane through the top of the building. A detector is placed at the coordinates $(x_d, y_d, h_s - h_d)$.

and the maximum polar angles are

$$\theta_{max} = \begin{cases} \tan^{-1}\left[\dfrac{x_2}{h_s \cos(\psi + \xi)}\right], \\ \qquad \psi_4 - 2\pi \le \psi \le \psi_1 , \\ \tan^{-1}\left[\dfrac{y_1}{h_s \cos(\psi + \xi - \pi/2)}\right], \\ \qquad \psi_1 \le \psi \le \psi_2 , \\ \tan^{-1}\left[\dfrac{x_1}{h_s \cos(\psi + \xi - \pi)}\right], \\ \qquad \psi_2 \le \psi \le \psi_3 , \\ \tan^{-1}\left[\dfrac{y_2}{h_s \cos(\psi + \xi - 3\pi/2)}\right], \\ \qquad \psi_3 \le \psi \le \psi_4 . \end{cases} \quad (23)$$

Two roofless rectangular building skyshine problems involving point isotropic monoenergetic neutron sources (14 and 3.25 MeV) were analyzed using the MCNP code. The dimensions of the room ($x \times y$) were 3048 × 4572 cm (100 × 150 ft). The source was located on the z axis at 0.5 m below the top of the wall, with $x_1 = x_2$ and $y_1 = y_2$. The detector was placed at the same elevation as the source. The skyshine dose as a function of x_d (with $y_d = 0$ m) was then evaluated. The MCNP results are presented, together with the integral line-beam method results, in Fig. 8. It can be seen that the integral line-beam method results agree very well with the MCNP results. As before, the integral line-beam method results are slightly higher than the MCNP results for $x \le 300$ m. Because small tally volumes were used in the MCNP calculations, the MCNP results for the secondary-photon dose for the 3.25-MeV neutron source were not reliable, and hence the results for these photons are not shown in Fig. 8.

III.D. Infinite-Air Geometry

The last skyshine problem analyzed using the integral line-beam method is for a 14-MeV point isotropic neutron source in an infinite-air medium as described in Ref. 19. The total dose at a detector for this case is the sum of the uncollided and the collided doses. A simple computer program was written to calculate the uncollided neutron dose. The collided dose was evaluated using the integral line-beam method for the open-silo geometry with a 14-MeV source at the top of the silo (2π geometry). The same problem was also analyzed using the MCNP code. The two sets of results are presented in Fig. 9, which illustrates the excellent agreement between the results.

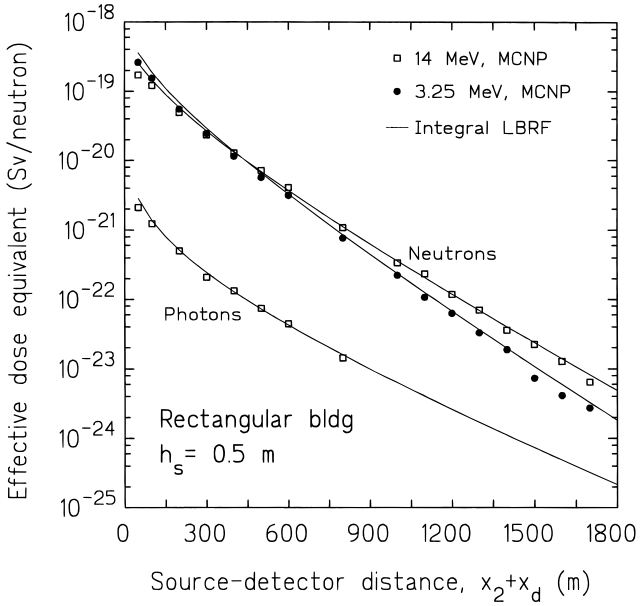

Fig. 8. Comparison of the MCNP (symbols) and the integral line-beam method results (lines) for the roofless rectangular room.

IV. CONCLUSIONS

To demonstrate the application of the integral line-beam method for neutron skyshine problems, four skyshine problems involving simple geometries were

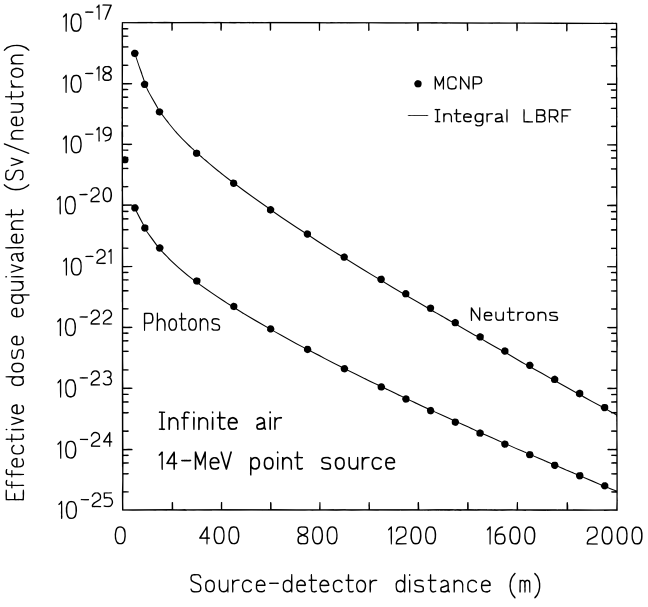

Fig. 9. Comparison of the MCNP and the integral line-beam method results for a 14-MeV point isotropic neutron source in an infinite-air geometry.

analyzed using the integral line-beam method. The geometries considered are (a) a source in an open silo, (b) a source behind an infinite wall, (c) a source inside a roofless rectangular building, and (d) a source in an infinite-air medium. The integral line-beam method results agree very well with the MCNP calculations for the same problems and were obtained at a fraction of the computational expense required by MCNP (typically seconds versus many hours or even days for MCNP). Thus, for routine neutron skyshine analyses, the integral line-beam method is an attractive alternative to the more involved transport techniques.

ACKNOWLEDGMENT

The extension of the line-beam skyshine method to neutron skyshine sources was partially supported by the Engineering Experiment Station at Kansas State University.

REFERENCES

1. C. M. LAMPLEY, "The Skyshine-II Procedure: Calculation of the Effects of Structure Design on Neutron, Primary Gamma Ray and Secondary Gamma Ray Dose Rates in Air," RRA-T7901 (NUREG/CR-0781), Radiation Research Associates (1979).

2. C. M. LAMPLEY, M. C. ANDREWS, and M. B. WELLS, "The SKYSHINE-III Procedure: Calculation of the Effects of Structure Design on Neutron, Primary Gamma-Ray and Secondary Gamma-Ray Dose Rates in Air," RRA T8209A (RSIC Code Collection CCC-289), Radiation Research Associates (1988).

3. "MicroSkyshine User's Manual," Grove Engineering, Rockville, Maryland (1987).

4. J. K. SHULTIS, R. E. FAW, and M. S. BASSETT, "The Integral Line-Beam Method for Gamma Skyshine Analysis," *Nucl. Sci. Eng.*, **107**, 228 (1991).

5. M. S. BASSETT, "Gamma Skyshine Calculations for Shielded Source," MS Thesis, Kansas State University, Department of Nuclear Engineering (1989).

6. J. K. SHULTIS, R. E. FAW, and X. DENG, "Improved Response Functions for Gamma-Ray Skyshine Analyses," SAND92-7296, Sandia National Laboratories (1992).

7. J. K. SHULTIS and R. E. FAW, "Extensions to the Integral Line-Beam Method for Gamma-Ray Skyshine Analyses," SAND94-2019, Sandia National Laboratories (1995).

8. F. A. KHAN, "Gamma-Ray Skyshine LBRF Near an Air-Ground Interface," MS Thesis, Kansas State University (1995).

9. A. A. GUI, J. K. SHULTIS, and R. E. FAW, "Application of the Integral Line-Beam Method to Neutron Skyshine Analysis," *Proc. Topl. Mtg. Radiation Protection and Shielding*, Vol. 2, p. 820, Falmouth, Massachusetts, April 21–25, 1996, American Nuclear Society (1996).

10. A. A. GUI, J. K. SHULTIS, and R. E. FAW, "Response Functions for Neutron Skyshine Analysis," *Nucl. Sci. Eng.*, **125**, 111 (1997).

11. J. K. SHULTIS and R. E. FAW, "Response Functions for Neutron and Gamma-Ray Skyshine Analysis," Report 271, Kansas State University, Engineering Experiment Station (1995); see also DLC-188/SKYDATA-KSU, Radiation Shielding Information Center, Oak Ridge National Laboratory.

12. A. A. GUI, "Response Functions for Neutron Skyshine Analysis," PhD Dissertation, Kansas State University (1994).

13. "Data for Use in Protection Against External Radiation," *Annals of the ICRP*, Vol. 17, No. 2/3, Publication 51, International Commission on Radiological Protection, Pergamon Press, Oxford, United Kingdom (1987).

14. "MCNP: A General Monte Carlo Code for Neutron and Photon Transport, Version 3A," LA-7396-M, Rev. 2, J. F. BRIESMEISTER, Ed., Los Alamos National Laboratory (1991).

15. J. K. SHULTIS, R. E. FAW, and F. S. KHAN, "SKYNEUT: A Code for Neutron Skyshine Calculations Using the Integral Line Beam Method," Report 9503, Institute for Computational Research in Engineering and Science, Kansas State University (1995); see also CCC-646/SKYSHINE-KSU, Radiation Shielding Information Center, Oak Ridge National Laboratory.

16. "Gamma-Ray Attenuation Coefficients and Buildup Factors for Engineering Materials," ANSI/ANS-6.4.3, American Nuclear Society (1991).

17. "Statement from the 1985 Paris Meeting of the International Commission on Radiological Protection," Publication 45, International Commission on Radiological Protection, Pergamon Press, Oxford, United Kingdom (1985).

18. "Protection Against Neutron Radiation," Report 38, National Council on Radiation Protection and Measurements, Washington, D.C. (1971).

19. E. A. STRAKER, "Shielding Benchmark Problem 3.0, Neutron Spectrum from Point Fission and 14-MeV Sources in Infinite Air," ORNL-RSIC-(ANS-SD-9), Oak Ridge National Laboratory (1970).